·临床研究·

MRI敷霜征鉴别乳腺良恶性小肿块的价值及其病理组织学分析

赖　婵[1]，刘壮盛[1]，李儒琼[1]，梁克明[1]，龙晚生[1]，李海成[2]，聂中新[1]
(1. 江门市中心医院//中山大学附属江门医院放射科，广东 江门 529070；2. 江门市中心医院//中山大学附属江门医院病理科，广东 江门 529070)

摘　要：【目的】探讨MRI敷霜征鉴别乳腺良恶性小肿块的价值，并分析其病理组织学改变。【方法】回顾性收集2016年6月~2020年9月我院行MRI检查并经病理证实的554例最大径线≤2 cm的乳腺小肿块患者资料(恶性291例，良性263例)。将患者的临床和MR特征进行单因素及多因素回归分析，筛选乳腺癌独立危险因素。基于独立危险因素构建两个诊断模型(模型1包含敷霜征，模型2不包含敷霜征)。采用ROC曲线评估两个模型的诊断效能。观察所有小肿块瘤周组织的病理学改变，分析敷霜征的病理学基础。【结果】恶性组199例(68.4%)、良性组25例(9.5%)出现敷霜征，两组间差异具有统计学意义($P<0.05$)。单因素及多因素回归分析显示，年龄、病灶径线、边缘、ADC值、时间-信号强度曲线类型、敷霜征为乳腺癌的独立危险因素，OR估计值分别为1.065、4.515、2.811、0.013、3.487和13.894，OR 95%CI分别为(1.034，1.097)、(2.368，8.608)、(1.954，4.045)、(0.004，0.049)、(2.087，5.826)和(7.026，27.477)。模型1(包含敷霜征)对乳腺小肿块的鉴别诊断效能优于模型2(不包含敷霜征)(AUC：0.938 *vs.* 0.897，$P<0.05$)。病理组织学分析显示敷霜征与瘤周炎性细胞浸润、血管增生相关。【结论】MRI敷霜征有助于乳腺良恶性小肿块的鉴别诊断，其病理组织学基础可能为瘤周炎性细胞浸润、血管增生。

关键词：磁共振成像；敷霜征；乳腺小肿块；良恶性；病理组织学
中图分类号：R445.2　　**文献标志码**：A　　**文章编号**：1672-3554(2022)02-0321-10
DOI：10.13471/j.cnki.j.sun.yat-sen.univ(med.sci).20211227.001

The Value of Blooming Sign on MRI in Distinguishing Malignancy from Benign Small Breast Masses and Its Radiologic-pathologic Correlation Analysis

LAI Chan[1], LIU Zhuang-sheng[1], LI Ru-qiong[1], LIANG Ke-ming[1], LONG Wan-sheng[1], LI Hai-cheng[2], NIE Zhong-xin[1]
(1. Department of Radiology, Jiangmen Central Hospital//The Affiliated Jiangmen Hospital of Sun Yat-sen University, Jiangmen 529070, China; 2. Department of Pathology, Jiangmen Central Hospital//The Affiliated Jiangmen Hospital of Sun Yat-sen University, Jiangmen 529070, China)
Correspondence to: LIU Zhuang-sheng; E-mail: zhuangshengliu@126.com

Abstract: 【Objective】 To determine the value of MRI blooming sign in differentiating benign and malignant small breast masses and investigate its radiologic-pathologic correlation. 【Methods】 This retrospective study included 554 small breast masses (291 malignant and 263 benign) which were ≤ 2 cm and validated by pathology analysis between June 2016 and September 2020. All 554 patients underwent breast MRI. The clinical characteristics and MR features were analyzed. Univariate and multivariate regression analysis were performed to identify the independent risk factors of breast cancer. Two diagnostic models were constructed based on independent risk factors (model 1 included blooming sign and model 2

收稿日期：2021-09-28
基金项目：江门市医疗卫生领域科技计划项目(2020YLA072)；江门市科技计划项目(江科[2015]73号第68项)；广东省医学科研基金(A2020622)；江门市中心医院科研杰青项目(J201904)
作者简介：赖婵，主治医师，研究方向：乳腺影像诊断，E-mail：392252609@qq.com；刘壮盛，通信作者，主任医师，研究方向：乳腺影像诊断，E-mail：zhuangshengliu@126.com

didn't). ROC curve was used to evaluate the diagnostic performances of the two models. The histological changes of peritumoral tissues in all small masses were analyzed.【Results】The blooming sign was positive in 199 cases (68.4%) of the malignant masses and 25 cases (9.5%) of the benign ones ($P<0.05$). Univariate and multivariate regression analysis showed that age, lesion diameter, margin, ADC value, time signal intensity curve type and blooming sign were independent risk factors for breast cancer. Odds ratio were 1.065, 4.515, 2.811, 0.013, 3.487 and 13.894, respectively. Their corresponding 95%CI were (1.034, 1.097), (2.368, 8.608), (1.954, 4.045), (0.004, 0.049), (2.087, 5.826) and (7.026, 27.477), respectively. The diagnostic performance of model 1 (blooming sign included) was better than that of model 2 (blooming sign not included; AUC: 0.938 *vs* 0.897, $P < 0.05$). Histopathological analysis showed that the blooming sign was related to peritumoral lymphocyte infiltration and vascular proliferation.【Conclusions】MRI blooming sign is helpful for distinguishing breast cancer from benign masses. The correlated histopathological basis may be peritumoral lymphocyte infiltration and neovascularization.

Key words: magnetic resonance imaging; blooming sign; small breast masses; benign and malignant; histopathology

[J SUN Yat-sen Univ(Med Sci),2022,43(2):321-330]

乳腺癌已成为全球女性发病率第一的恶性肿瘤[1]。在乳腺癌筛查过程中,乳腺小肿块(≤2 cm)的发现率越来越高[2]。如何有效鉴别乳腺良恶性小肿块,减少不必要的活检,减轻患者的心理负担,是临床实践中亟待解决的关键问题[1,3-5]。随着乳腺MRI的普及,MRI征象鉴别乳腺良恶性肿块的研究也越来越深入[6],除了关注肿块本身的特征以外,越来越多的研究开始关注瘤周组织的影像学改变对肿瘤的定性作用[7-8]。Fischer[9]提出MRI敷霜征(blooming sign, BS)可以反映瘤周间质改变,是鉴别乳腺良恶性肿块的重要MR征象之一。然而,目前国内尚未见关于此征象的报道。因此,笔者对本院554例经手术病理证实的乳腺小肿块患者临床资料、MRI特征及病理切片进行回顾性分析,旨在评价MRI敷霜征对乳腺小肿块的定性诊断价值并分析其病理组织学基础。

1 材料与方法

1.1 研究对象

本研究经我院医学伦理会批准,符合免除知情同意的条件。回顾性收集2016年6月~2020年9月于我院行MRI检查并经病理组织证实的肿块型乳腺病灶的患者资料。纳入标准:①病变为肿块型,最大径线≤2 cm;②MR扫描前未进行治疗或活检;③有手术病理结果。排除标准:①非肿块型病变;②乳腺炎性病变;③最大径线>2 cm;④检查前已行活检或治疗;⑤MRI图像伪影严重。按上述标准,共纳入554例小肿块型乳腺病灶,其中恶性291例,良性263例;患者年龄(51.9±10.3)岁(范围23~74岁)。

1.2 MRI检查

检查前训练患者平静呼吸,以最大限度减少运动伪影。未绝经患者于月经周期7~10天检查。

采用Philips Ingenia 3.0 T超导型扫描仪,7通道乳腺专用线圈。取俯卧位,扫描范围为双侧乳腺及腋窝。扫描参数:①轴位T1WI:TR 520 ms,TE 1.93 ms,层厚4 mm,层间距0.5 mm,矩阵312×397,FOV 280 mm×357 mm。②轴位T2WI压脂序列:TR 4 355 ms,TE 60 ms,层厚4 mm,层间距0.5 mm,矩阵312×379,FOV 280 mm×358 mm。③扩散加权图像DWI:采用单次激发平面回波成像技术(SE-EPI),b值取50和800 s/mm^2,TR 4765 ms,TE 60.0 ms,层厚4 mm,层间距0.5 mm,矩阵100×120,FOV 280 mm×340 mm。④动态增强扫描采用3D THRIVE序列,1期蒙片+6期增强。每期扫描时间约80 s。对比剂GD-DTPA,剂量0.2 mmol/kg,注射流速2.0 mL/s。注药60 s后启动6期动态增强扫描。

图像后处理:取增强后第6期的图像与增强后第1期的图像进行减影,得到延迟期减影图像。用后处理软件测量肿块ADC值,绘制时间信号强度曲线(time signal intensity curve, TIC)。

1.3　图像分析

由两位具有5年以上乳腺MRI诊断经验医生对患者MRI图像进行评估，意见不一致时通过协商讨论解决分歧。患者具有多发病灶时，只选取其中径线最大的病灶进行分析。观察病灶的MRI特征：①径线（横断位最大层面长径）；②位置（外上象限、外下象限、内上象限、内下象限、中央区）；③形状（圆形、卵圆形、不规则）；④边缘（清晰、分叶、毛刺）；⑤T_2WI信号（与同侧正常腺体对比：低信号、等信号、高信号）；⑥ADC值（取病灶内最低ADC值）；⑦内部强化特征（无强化、均匀强化、不均匀强化）；⑧TIC曲线类型（time signal intensity curve）（流入型、平台型、流出型）；⑨敷霜征（无或有；敷霜征指MRI动态增强早期图像上病变边缘清楚锐利，随着时间的延迟，病灶的范围逐渐扩大，边缘也逐渐变得模糊；延迟期减影图像上瘤周乳腺组织见环状、斑片状高信号影[10]）；⑩纤维腺体组织类型（fibro glandular tissue composition，FGT）（a：脂肪型、b：少量纤维腺体型、c：不均匀致密型、d：极度致密型）；⑪乳腺背景实质强化（background parenchymal enhancement，BPE；轻微、轻度、中度、明显）。

1.4　病理组织学分析

所有病理切片均由同一位具有丰富乳腺病理诊断经验的医生进行分析。手术切除的乳腺小肿块标本以2～3 mm的间隔进行切片，行HE染色，在常规光学显微镜下进行评估。观察肿块周围乳腺组织的病理学改变：①纤维组织增生（无或有）；②炎性细胞浸润（无、少量、大量）；③新生血管形成（无或有）；④出血（无或有）；⑤坏死（无或有）；⑥囊变（无或有）。

1.5　统计学分析

采用R3.4.4、SPSS 22.0和Matlab2018b统计学软件分析，$P<0.05$表示差异具有统计学意义。计量资料采用均数±标准差表示；符合正态分布且方差齐性的定量资料（年龄、径线）采用两组独立样本t检验，方差不齐的资料（ADC值）采用校正t检验；定性资料（位置、形状、边缘、T_2WI信号、内部强化特征、TIC曲线类型、敷霜征、乳腺纤维腺体类型、乳腺背景强化程度、纤维组织增生、炎性细胞浸润、新生血管形成、出血、坏死、囊变）采用Pearson χ^2检验。

对临床资料、MRI特征进行单因素和多因素Logistic回归分析，筛选乳腺癌的独立危险因素。基于独立危险因素，通过Logistic回归构建两个诊断模型，其中模型1包含敷霜征，模型2不包含敷霜征。

采用受试者工作特征（receiver operating characteristic，ROC）曲线评估两个诊断模型鉴别乳腺良恶性小肿块的效能。分别计算两个模型的曲线下面积（area under the curve，AUC）、敏感度、特异度、准确度。采用Delong检验比较两个诊断模型的AUC值差异。

2　结　果

2.1　临床、MRI特征

554例乳腺小肿块中恶性291例，良性263例，具体病理组织学分型见表1。

表1　乳腺小肿块病理组织类型

Table 1　Pathological types of small breast masses

Pathological types	n(%)
Benign (n=263)	
Fibroadenoma	114(43.34)
Lobular hyperplasia	9(3.42)
Cyst	43(16.35)
Intraductal papilloma	61(23.19)
Benign phyllodes tumor	13(4.94)
Mammary gland disease	23(8.75)
Malignant (n=291)	
Nonspecific invasive carcinoma	203(69.76)
Invasive micropapillary carcinoma	22(7.56)
Invasive lobular carcinoma	18(6.19)
Ductal carcinoma in situ	17(5.84)
Mucinous carcinoma	31(10.65)

恶性组患者年龄（48.6±10.5）岁大于良性组（42.2±10.7）岁（t = −6.948，P < 0.001；表2）。恶性组径线（14.8±4.3）mm大于良性组（9.5±4.5）mm（t = −14.199，P < 0.001；表2）。

表2 良性组及恶性组临床特征和MRI特征比较

Table 2 Comparison of the clinical and MRI characteristics between benign and malignant small breast masses

Characteristics	Benign(n=263)	Malignant(n=291)	t/χ^2	P
Age/years	42.2±10.7	48.6±10.5	−6.948	<0.001
Menopausal status			2.960	0.085
Premenopausal	70	97		
Postmenopausal	193	194		
Lactation history			2.462	0.117
Absent	31	23		
Present	232	268		
Size/mm	9.5±4.5	14.8±4.3	−14.199	<0.001
Tumor location			8.090	0.088
Outer upper quardrant	68	50		
Outer lower quadrant	57	82		
Inner upper quadrant	57	69		
Inner lower quadrant	41	51		
Central area	40	39		
Margin			158.209	<0.001
Sharp	167	60		
Lobulated	81	89		
Spiculated	14	55		
Lobulated & Spiculated	1	87		
Shape			1.822	0.177
Round & oval	197	203		
Irregular	66	88		
ADC value/($\times10^{-3}$mm^2/s)	1.38±0.31	1.11±0.19	11.930	<0.001
T_2WI			0.751	0.687
Low	36	35		
Medium	8	12		
High	219	244		
Internal enhancement pattern			60.117	<0.001
Absent	43	3		
Homogeneous	132	121		
Heterogeneous	88	167		
TIC type			121.883	<0.001
Persistent	55	31		
Plateau	186	109		
Washout	22	151		
Blooming sign			198.847	<0.001
No	238	92		
Yes	25	199		
FGT			0.046	0.829

续表

Characteristics	Benign（n=263）	Malignant（n=291）	t/χ^2	P
A & B	67	71		
C & D	196	220		
BPE			0.393	0.531
Minimal & mild	189	216		
Moderate & marked	74	75		

FGT：Fibro glandular tissue composition；BPE：Background parenchymal enhancement.

敷霜征在恶性组（199/291，68.4%）出现的频率高于良性组（25/263，9.5%；χ^2= 198.847，P<0.001；表2；图1~3），其单独诊断乳腺癌的敏感度为68.8%，特异度为82.1%。病灶边缘特征、ADC值、内部强化特征、TIC曲线类型在良恶性组间差异具有统计学意义（P均<0.001；表2）。

2.2　独立危险因素筛选

单因素Logistic回归分析显示，年龄、病灶径线、边缘特征、ADC值、内部强化特征、TIC曲线类型、敷霜征在良恶性组间具有统计学差异（P均<0.05），年龄OR 95%CI为1.058（1.040，1.077）、病灶径线OR 95%CI为11.473（7.434，17.707）、边缘特征OR 95%CI为3.886（3.034，4.979）、ADC值OR 95%CI为0.012（0.005，0.030）、内部强化特征OR 95%CI为2.935（2.185，3.943）、TIC曲线类型OR 95%CI为4.040（2.960，5.513）、敷霜征OR 95%CI为20.592（12.736，33.294）。

多因素逻辑回归分析（表3）显示，年龄、病灶径线、边缘特征、ADC值、TIC曲线类型、敷霜征为乳腺癌的独立危险因素，年龄OR 95%CI为1.065（1.034，1.097）、病灶径线OR 95%CI为4.515（2.368，8.608）、边缘特征OR 95%CI为2.811（1.954，4.045）、

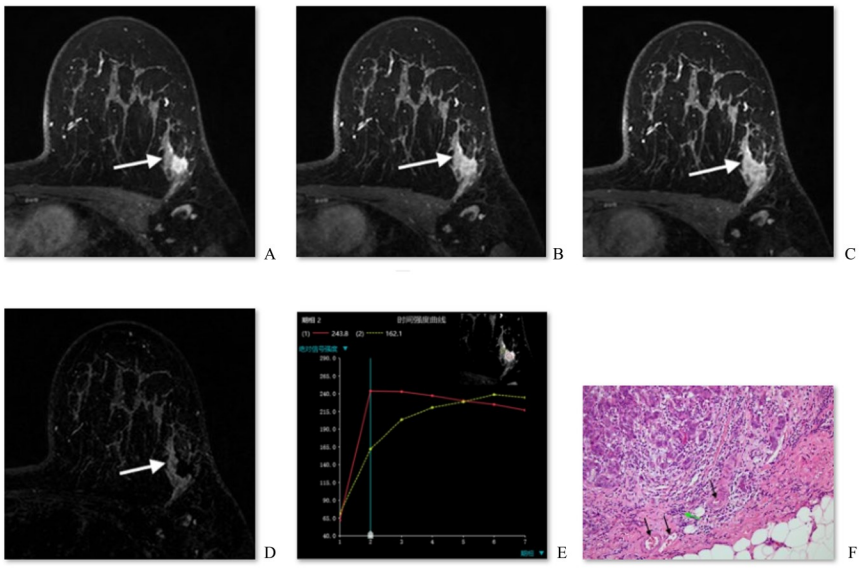

A 45-year-old woman with left breast pain during menstrual period for about 3 years. A-C: Blooming sign. The 1st, 3rd and 6th post-contrast images of dynamic contrast-enhance showed that the margin of the mass was sharp in early phase, and gradually blurred and expanded in the delay phase, especially in the 6th phase (white arrow). D: Subtraction image (6th phase minus 1st phase) showed that the peritumoral area illustrated delayed enhancement (white arrow). E: Time-signal intensity curve showed washout curve in tumor area and persistent curve in peritumoral area. F: Pathological image showed a nonspecific invasive carcinoma, surrounded by a large number of inflammatory cell (green arrow), fibrous tissue hyperplasia and neovascularization (black arrow, HE:×100).

图1　敷霜征阳性患者1 MRI表现及病理图像

Fig. 1　MRI features and pathological change in patient 1 with positive blooming sign

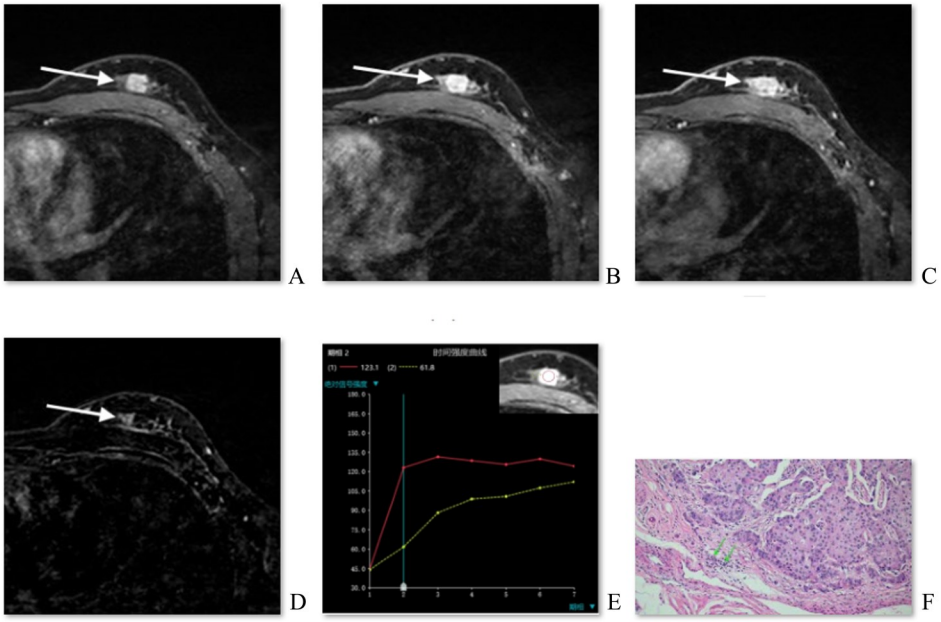

A 44-year-old woman with left breast mass in breast cancer screening. A-C: Blooming sign. The 1st, 3rd and 6th post-contrast images of dynamic contrast-enhance showed that the margin of the mass was sharp in 1st phase and gradually blurred and expanded in the delay phase, especially in 6th phase (white arrow). D: Subtraction image (6th phase minus 1st phase) showed that the peritumoral area illustrated delayed enhancement (white arrow). E: Time-signal intensity curve showed platform type in tumor area and persistent type in peritumoral area. F: Pathological image showed a nonspecific invasive carcinoma, surrounded by a certain number of inflammatory cell (green arrow), fibrous tissue hyperplasia (HE:×100).

图2 敷霜征阳性患者2 MRI表现及病理图像

Fig. 2 MRI features and pathological images in patient 2 with positive blooming sign

ADC值OR 95%CI为0.013(0.004, 0.049)、TIC曲线类型OR 95%CI为3.487(2.087, 5.826)、敷霜征OR 95%CI为13.894(7.026, 27.477)。

2.3 诊断模型构建及诊断效能比较

基于年龄、病灶径线、边缘特征、ADC值、TIC曲线类型、敷霜征6个危险因素构建模型1,基于年龄、病灶径线、边缘特征、ADC值、TIC曲线类型5个危险因素构建模型2。

ROC曲线分析显示,模型1(含敷霜征)AUC值为0.938,准确度85.2%,敏感度77.0%,特异度

表3 多因素Logistic回归分析

Table 3 Multivariable logistic regression analyses

Variables	b	S_b	Wald χ^2	P	$\widehat{OR}$	OR 95%CI
Constant	−4.703	1.149	16.757	<0.001	0.009	
Age	0.063	0.015	17.659	<0.001	1.065	1.034, 1.097
Size	1.507	0.329	20.959	<0.001	4.515	2.368, 8.608
Margin	1.034	0.186	31.001	<0.001	2.811	1.954, 4.045
ADC value	4.310	0.657	43.079	<0.001	0.013	0.004, 0.049
TIC type	1.249	0.262	22.747	<0.001	3.487	2.087, 5.826
BS	2.631	0.348	57.207	<0.001	13.894	7.026, 27.477
Internal enhancement pattern	0.389	0.257	2.292	0.130	1.476	0.892, 2.442

Multivariable analysis was performed by using the variables showing a P value <0.05 at univariable analysis; TIC: time signal intensity curve; BS: blooming sign.

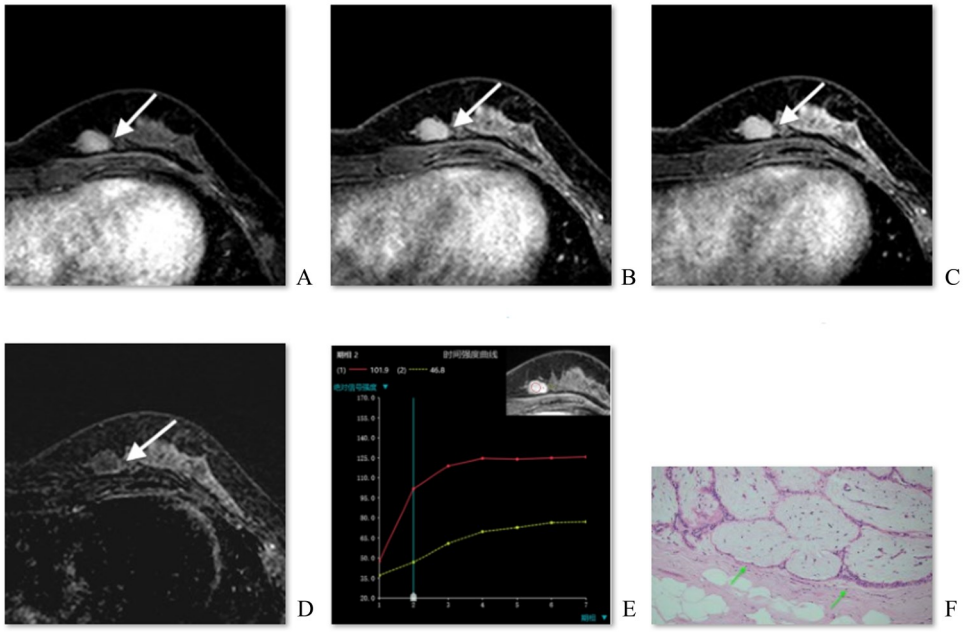

A 52-year-old woman with left breast mass in breast cancer screening. A-C: No blooming sign. The 1st, 3rd and 6th post-contrast images of dynamic contrast-enhance showed that the margin of the mass was smooth and clear, without peritumoral delayed enhancement (white arrow). D: Subtraction image (6th phase minus 1st phase) showed no delayed enhancement in the peritumoral area (white arrow). E: Time-signal intensity curve showed platform type in tumor area and persistent type in peritumoral area. F: Pathological image showed a fibroadenoma, surrounded by fibrous tissue hyperplasia, a small amount inflammatory cells (green arrow, HE:×100).

图3　敷霜征阴性患者MRI表现及病理图像

Fig. 3　MRI features and pathological images in a patient with negative blooming sign

94.3%，PPV 93.7%，NPV 78.7%；模型2（不包含敷霜征）AUC值为89.7%，准确度82.5%，敏感度83.2%，特异度81.8%，PPV 83.5%，NPV 81.4%。模型1的AUC值高于模型2（$Z=4.658$，$P<0.001$；图4）。

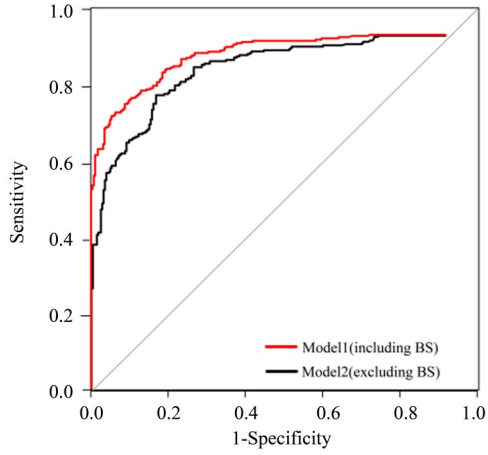

图4　两个模型的ROC曲线分析

Fig. 4　Receiver operating characteristic analysis of model 1 and model 2

2.4　病理组织学分析

554例乳腺小肿块中，敷霜征阳性共236例（恶性211例，良性25例），敷霜征阴性共318例（恶性80例，良性238例）。瘤周病理组织分析显示，敷霜征阳性组小肿块周围炎性细胞浸润（$\chi^2=149.345$，$P<0.001$）及新生血管形成（$\chi^2=84.284$，$P<0.001$，图1~3）较敷霜征阴性组常见；而两组间瘤周纤维组织增生、出血、囊变、坏死的差异均无统计学意义（P均>0.05；表4）。

3　讨论

在乳腺癌筛查过程中，乳腺小肿块（≤2 cm）的发现率越来越高[2]。但由于乳腺小肿块的MRI特征存在一定的重叠，误诊率较高[10]。乳腺小肿块影像学的定性诊断已不仅仅限于瘤体本身的特征，瘤周乳腺组织的影像学改变对肿瘤的定性作用也得到越来越多的关注[7, 11-12]。Fischer[9]在乳腺肿块周围组织MRI信号改变的研究中，发现敷霜征

表4 敷霜征阳性及阴性组小肿块瘤周病理组织学改变

Table 4 Histopathologic changes of peritumoral area between BS positive and negative masses [n(%)]

Peritumoral changes	Blooming sign		χ^2	P
	+ (n=236)	− (n=318)		
Lymphocyte infiltration			149.345	<0.001
None	0(0)	67(21.1)		
Small amount	90(38.1)	202(63.5)		
Abundant	146(61.9)	49(15.4)		
Fibrous tissue hyperplasia			0.013	0.910
Small amount	79(33.5)	105(33.0)		
Abundant	157(66.5)	213(67.0)		
Neovascularization			84.284	<0.001
No	131(55.5)	285(89.6)		
Yes	105(44.5)	33(10.4)		
Bleeding			0.015	0.902
No	202(85.6)	271(85.5)		
Yes	34(14.4)	47(14.5)		
Cystic			0.028	0.866
No	214(90.7)	287(90.3)		
Yes	22(9.3)	31(9.7)		
Nescosis			0.034	0.854
No	190(80.5)	258(81.1)		
Yes	46(19.5)	60(18.9)		

(blooming sign, BS)可以作为乳腺良恶性小肿块的鉴别征象之一。该征象是指在MRI动态增强扫描早期,乳腺小肿块边缘锐利,随着时间延迟,病灶外缘逐渐变得模糊,周围乳腺组织内可出现环形、条索状、小斑片状延迟强化影。Fischer等[9]研究显示324例恶性肿块及41例良性肿块瘤周出现敷霜征,出现率分别为63.0%(324/514)、14.7%(41/279),诊断乳腺癌的敏感度为63.0%,特异度为85.3%。Dietzel等[13-14]研究认为敷霜征有助于直径小于5 mm的乳腺小病变的鉴别诊断。Kaiser等[15]研究显示敷霜征常见于乳腺恶性肿块,较少见于良性肿块,对乳腺癌的诊断具有较高的特异性(特异度93.2%,OR 9.7)。本研究显示,554例最大径线≤2 cm的乳腺小肿块中,恶性组有199例(68.4%)、良性组有25例(9.5%)瘤周出现敷霜征。敷霜征与乳腺恶性小肿块有较高的相关性,其单独诊断乳腺癌的敏感度为68.8%,特异度为82.1%,与既往研究结果大致相符。但本研究中良性组敷霜征的发生率低于Fischer等[9]所报道的结果,可能与本研究入组标准为最大径≤2 cm的肿块型病变,排除了直径超过2 cm或者非肿块型病变有关。

此外,本研究单因素分析显示年龄、病灶径线、边缘特征、ADC值、内部强化特征、TIC曲线类型对乳腺小肿块的鉴别诊断均具有统计学意义(P均<0.05),研究结果与文献报道相符合[2, 4]。本研究进一步将上述具有鉴别诊断价值的乳腺MRI常见特征及敷霜征纳入多因素回归分析,结果显示年龄、病灶径线、边缘特征、ADC值、TIC曲线类型及敷霜征均为乳腺癌的独立危险因素。基于独立危险因素建立两个诊断模型,经ROC分析发现模型1(含敷霜征)较模型2(无敷霜征)的诊断效能更优(AUC 0.938 *vs.* 0.897,P<0.05),这也进一步说明MRI敷

霜征作为一种反映瘤周组织MRI信号改变的征象，与乳腺MRI常见特征结合，有助于提高乳腺小肿块的诊断效能，特别是提高了诊断的特异性。

目前，一些关于瘤周乳腺组织改变的基础性研究[8, 16]，可以解释MRI敷霜征的病理组织学改变。Houthuijzen等[8]研究发现肿瘤周围组织中存在大量的肿瘤相关性成纤维细胞，这是瘤周微环境的主要物理架构。这些成纤维细胞合成并分泌单核细胞趋化蛋白-1，促使大量淋巴细胞、中性粒细胞、巨噬细胞向肿瘤周围聚集，在瘤体周围形成瘤周间质反应带[17]。同时这些肿瘤相关性炎性细胞在处于缺氧状态下，合成并分泌促血管生成性趋化因子，如促血管生成因子，诱导瘤内及瘤周新生血管形成[18]。新生的血管排列较紊乱，壁薄，通透性较高，在增强扫描时高速团注对比剂，毛细血管内静水压增高，对比剂易外渗至瘤周间质内[9]。本研究对554例小肿块的瘤周病理分析结果显示，敷霜征阳性组与阴性组的瘤周均可见不同程度的纤维间质增生，包绕肿块，两组间无明显统计学差异（$P>0.05$）。敷霜征阳性组小肿块周围炎性细胞浸润（$\chi^2=149.345$，$P<0.001$）及新生血管形成（$\chi^2=84.284$，$P<0.001$）较敷霜征阴性组常见，且阳性组更常见大量炎性细胞（61.9% *vs.* 15.4%）及数量较多、形态较紊乱的新生血管（44.5% *vs.* 10.4%）。我们的研究结果与既往文献报道相符合。

本研究的局限性：①本研究为单中心回顾性研究，纳入的病例数有限，不可避免会存在选择偏倚及统计偏倚。②敷霜征属于一种主观定性征象，未将其进行客观量化研究，这是我们下一步研究的方向。③由于本研究纳入的单纯导管原位癌及三阴型乳腺癌的样本量有限，未能针对乳腺癌病理类型、分子分型与敷霜征的相关性进一步行分层分析，下一步我们继续收集病例，扩大样本量，补充这一方面的内容。

综上，乳腺MRI敷霜征作为一种反映瘤周间质改变的征象，有助于乳腺良恶性小肿块的鉴别诊断，与乳腺MRI常见特征相结合，可以提高诊断的特异性。敷霜征病理基础与瘤周组织炎性细胞浸润及新生血管形成有关。

参考文献

[1] Bray F, Ferlay J, Soerjomataram I, et al. Global cancer statistics 2018: GLOBOCAN estimates of incidence and mortality worldwide for 36 cancers in 185 countries [J]. CA Cancer J Clin, 2018, 68(6): 394-424.

[2] Kawai M, Kataoka M, Kanao S, et al. The value of lesion size as an adjunct to the BI-RADS-MRI 2013 descriptors in the diagnosis of solitary breast masses [J]. Magn Reson Med Sci, 2018, 17(3): 203-210.

[3] 汤易，李传乐，魏博文，等. 邻近血管征对BI-RADS 3、4类病变的诊断价值[J]. 影像诊断与介入放射学，2020，29(6)：421-425.
Tang Y, Li CL, Wei BW, et al. Value of adjacent vascular sign in the diagnosis of Breast Imaging Reporting and Data System category 3 and 4 lesions[J]. Diagn Imaging & Interv Radiol, 2020, 29(6): 421-425.

[4] Welch HG, Prorok PC, O'Malley AJ, et al. Breast-cancer tumor size, overdiagnosis, and mammography screening effectiveness [J]. N Engl J Med, 2016, 375(15): 1438-1447.

[5] Preibsch H, Wanner LK, Staebler A, et al. Malignancy rates of B3-lesions in breast magnetic resonance imaging- do all lesions have to be excised?[J]. BMC Medical Imaging, 2018, 18(1): 224-229.

[6] Yilmaz E, Sari O, Yilmaz A, et al. Diffusion-weighted imaging for the discrimination of benign and malignant breast masses; utility of ADC and relative ADC[J]. J Belg Soc Radiol, 2018, 102(1): 24-33.

[7] Heesch A, Maurer J, Stickeler E, et al. Development of radiotracers for breast cancer-the tumor microenvironment as an emerging target [J]. Cells, 2020, 9(10): 671-680.

[8] Houthuijzen JM, Jonkers J. Cancer-associated fibroblasts as key regulators of the breast cancer tumor microenvironment [J]. Cancer Metastasis Rev, 2018, 37(4): 577-597.

[9] Fischer DR, Baltzer P, Malich A, et al. Is the "bloom-

ing sign" a promising additional tool to determine malignancy in MR mammography?[J]. Eur Radiol, 2004, 14(3): 394-401.

[10] 孙恒翠, 甘洁, 郭依廷. 磁共振在乳腺小肿块病变良恶性鉴别诊断中的应用价值[J]. 医学影像学杂志, 2019, 29(11): 1909-1913.
Sun HC, Gan J, Guo YT. Diagnostic value of MRI in differential between benign and malignant of small masses[J]. J Med Imaging, 2019, 29(11):1909-1913.

[11] Baltzer PA, Dietzel M, Vag T, et al. Clinical MR mammography: impact of hormonal status on background enhancement and diagnostic accuracy [J]. Rofo, 2011, 183(5): 441-447.

[12] Zhang W, Shen Y, Huang H, et al. A rosetta stone for breast cancer: prognostic value and dynamic regulation of neutrophil in tumor microenvironment [J]. Front Immunol, 2020, 11:1779-1794.

[13] Dietzel M, Kaiser C, Baltzer PA. Magnetic resonance imaging of intraductal papillomas: typical findings and differential diagnosis [J]. J Comput Assist Tomogr, 2015, 39(2): 176-184.

[14] Dietzel M, Baltzer PA, Vag T, et al. Differential diagnosis of breast lesions 5mm or less is there a role for magnetic resonance imaging[J]. J Comput Assist Tomogr, 2010, 34(3): 456-464.

[15] Kaiser CG, Baltzer P, Kaiser AK, et al. The value of "constant sharpness" as a diagnostic sign in MR-Mammography[J]. Eur J Radiol Open, 2016, 3: 236-238.

[16] Sasada S, Shiroma N, Goda N, et al. The relationship between ring-type dedicated breast PET and immune microenvironment in early breast cancer [J]. Breast Cancer Res Treat, 2019, 177(3): 651-657.

[17] Joshi RS, Kanugula SS, Sudhir S, et al. The role of cancer-associated fibroblasts in tumor progression[J]. Cancers (Basel), 2021, 13(6): 450-461.

[18] De Francesco EM, Sims AH, Maggiolini M, et al. GPER mediates the angiocrine actions induced by IGF1 through the HIF-1α/VEGF pathway in the breast tumor microenvironment [J]. Breast Cancer Res, 2017, 19(1): 129-139.

(编辑 余 菁)